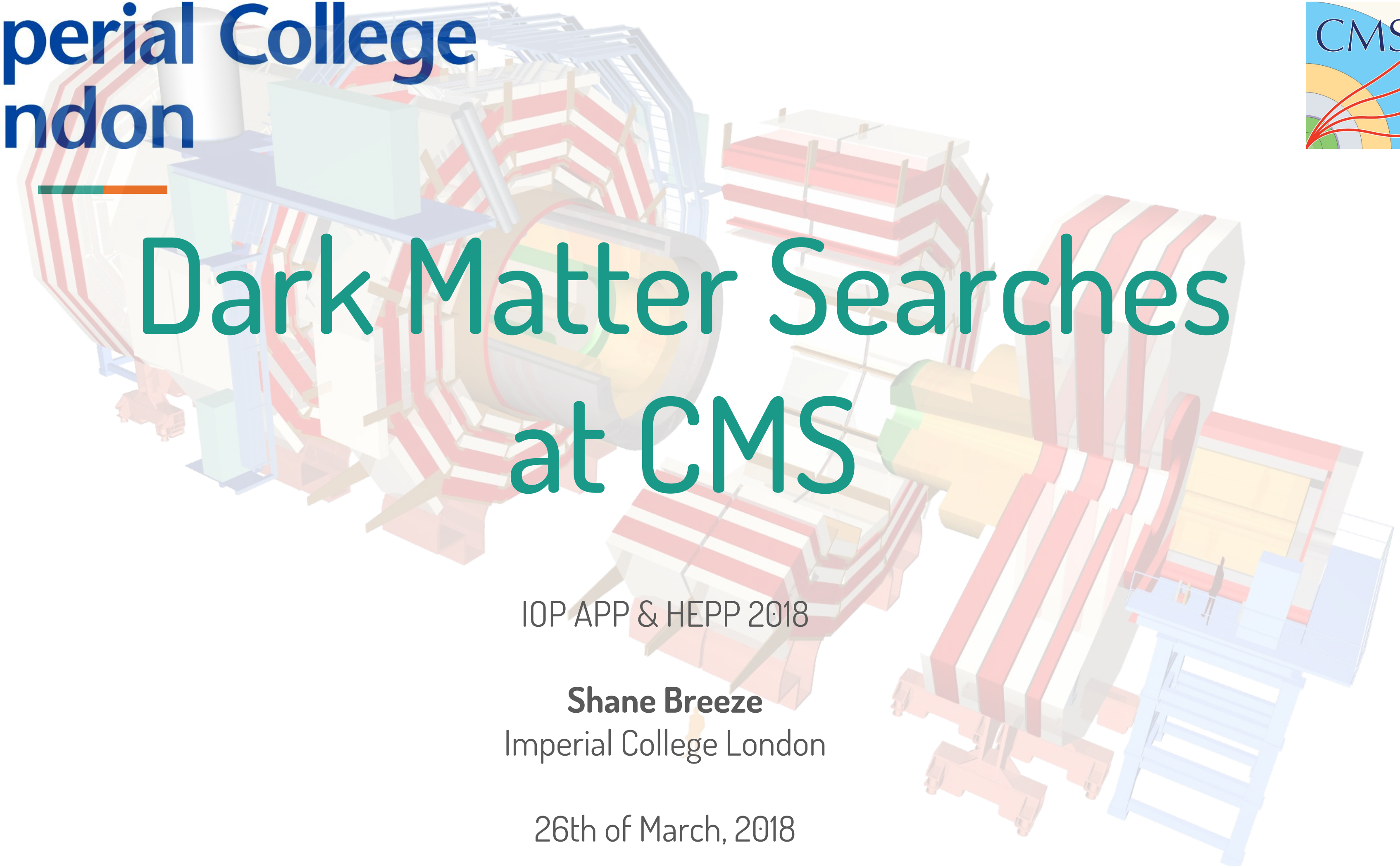

Dark Matter Searches at CMS

IOP APP & HEPP 2018

Shane Breeze
Imperial College London

26th of March, 2018

Motivations

Galaxies rotate too fast given their visible component

Rotation curves

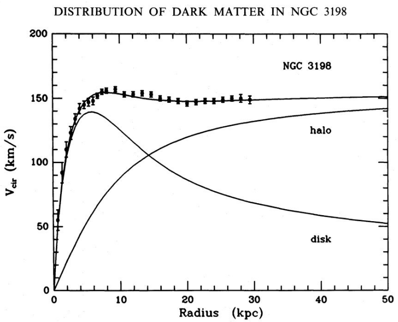

Motivations

Galaxies rotate too fast given their visible component

Rotation curves

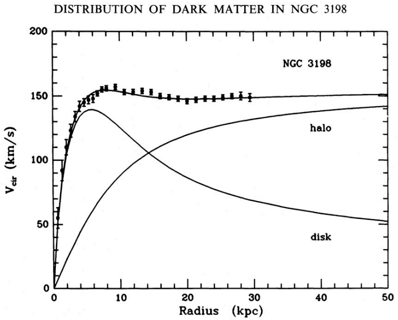

Cosmic Microwave Background

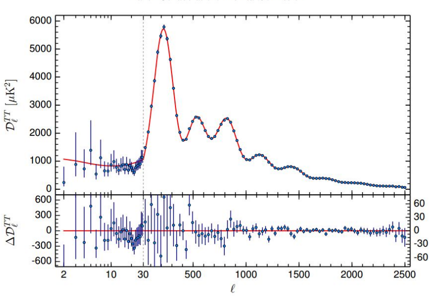

Oscillations in the hot gas of the early universe is highly dependent on the content of the universe

Motivations

Galaxies rotate too fast given their visible component

Rotation curves

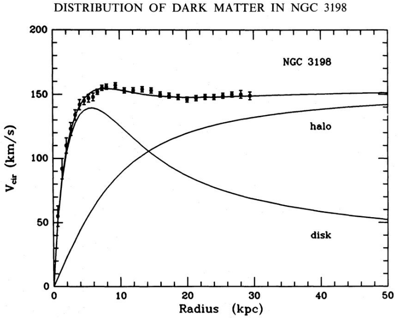

Cosmic Microwave Background

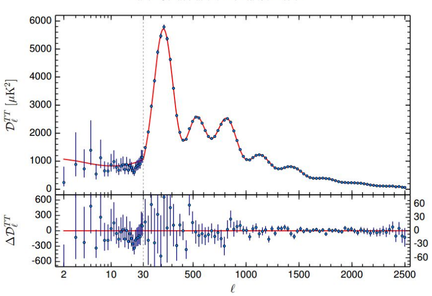

Oscillations in the hot gas of the early universe is highly dependent on the content of the universe

Gravitational Lensing

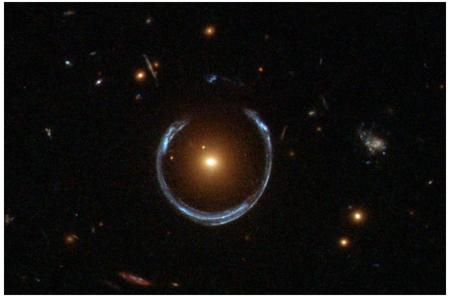

Galactic masses agree with the existence of a invisible massive component

Motivations

Galaxies rotate too fast given their visible component

Rotation curves

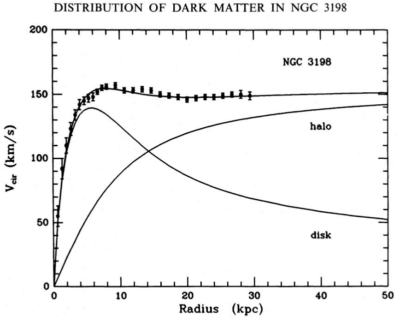

Cosmic Microwave Background

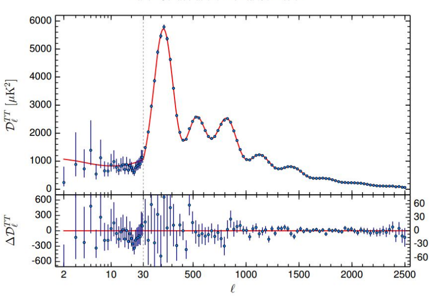

Oscillations in the hot gas of the early universe is highly dependent on the content of the universe

Galactic masses agree with the existence of a invisible massive component

Gravitational Lensing

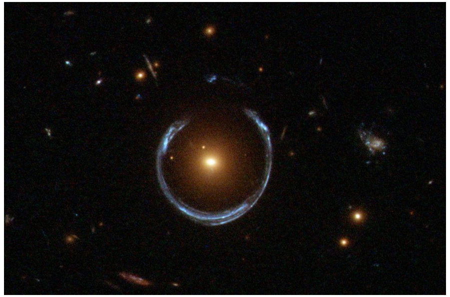

Bullet Cluster

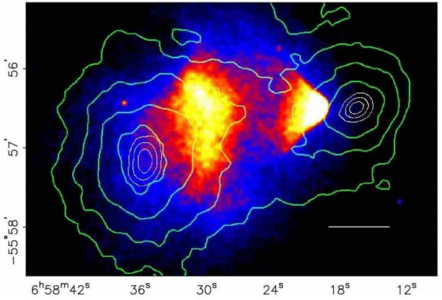

Separation of visible (x-rays) and invisible (gravitational lensing) components of collided galaxy clusters

Motivations

Galaxies rotate too fast given it's visible component

Galactic masses agree with the existence of a invisible massive component

WIMP miracle:

All of these observations can be explained by the existence of a weak scale particle, with masses from a few GeV to the TeV scale

The LHC directly probes these scales

Oscillations in the hot gas of the early universe is highly dependent on the content of the universe

Separation of visible (x-rays) and invisible (gravitational lensing) components of collided galaxy clusters

Dark Matter Signature

Simplified Dark Matter models form a credible unit of a complicated model and are easier to interpret

- Introduce a single mediator to couple the SM particle to the DM particles
- This mediator can be a vector, axial-vector, scalar or pseudoscalar particle

Dark Matter Signature

Simplified Dark Matter models form a credible unit of a complicated model and are easier to interpret

Light flavour production

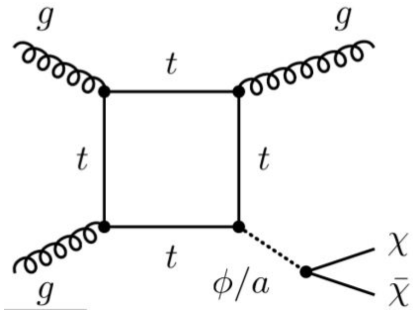

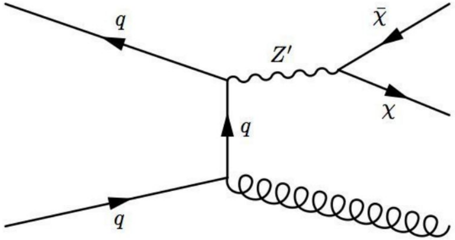

Dark Matter Signature

Simplified Dark Matter models form a credible unit of a complicated model and are easier to interpret

Light flavour production

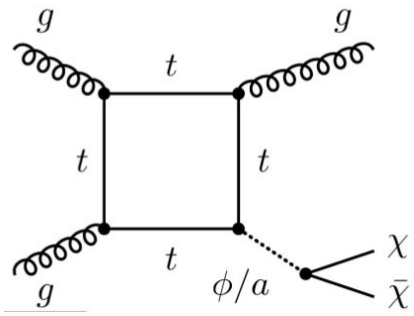

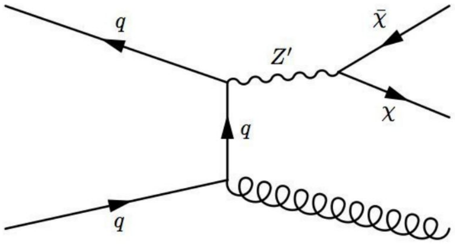

Heavy flavour production

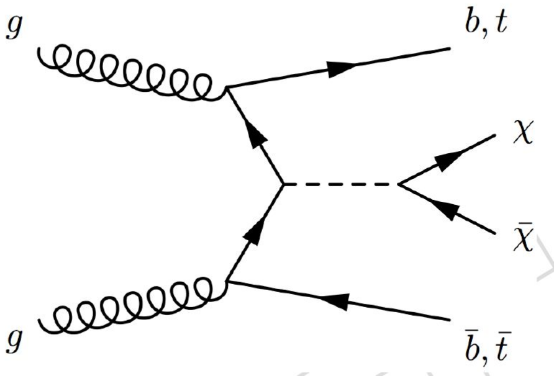

Analysis overview

Inclusive search for new physics in the MET+jets final state

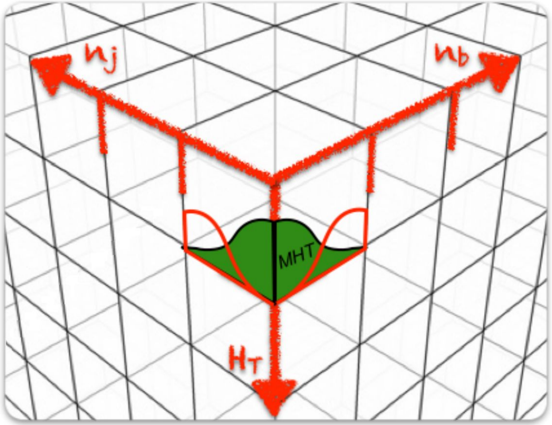

Analysis overview

Jet multiplicity (n_j):

- 1 or more jets from the initial state through radiation or the production mechanism

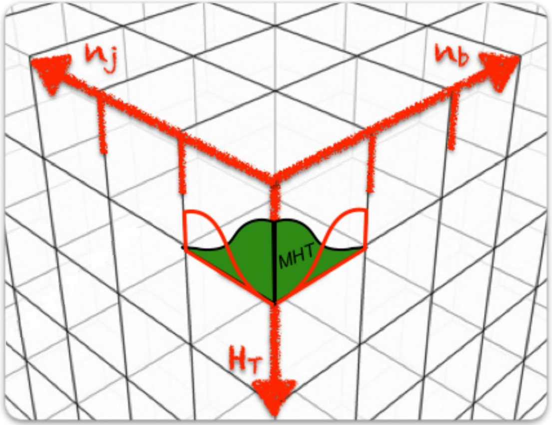

Analysis overview

Jet multiplicity (n_j):

- 1 or more jets from the initial state through radiation or the production mechanism

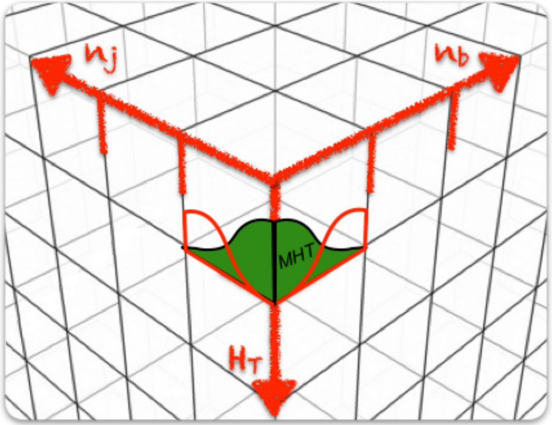

B-jet multiplicity (n_b):

- Target new physics produced in association to top or bottom quarks

Analysis overview

Jet multiplicity (n_j):

- 1 or more jets from the initial state through radiation or the production mechanism

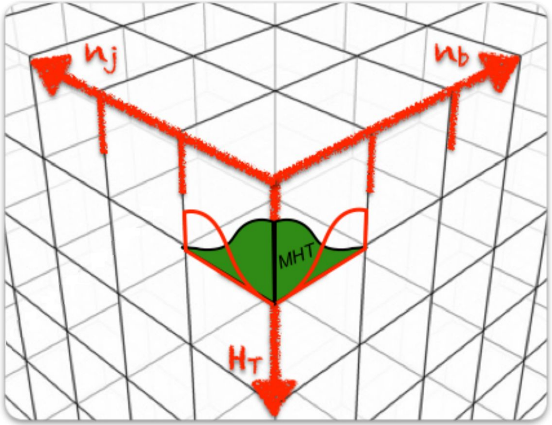

B-jet multiplicity (n_b):

- Target new physics produced in association to top or bottom quarks

Scalar sum of hadronic transverse energy (H_T)

- Probes various hadronic energy scales

Analysis overview

Missing hadronic transverse energy (*MHT*)

- Shape is sensitive to events with invisible particles

Jet multiplicity (n_j):

- 1 or more jets from the initial state through radiation or the production mechanism

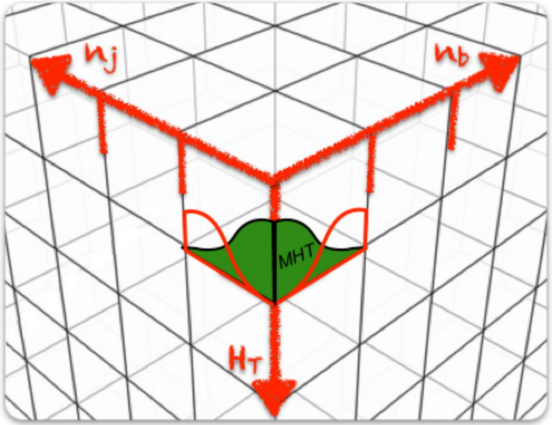

B-jet multiplicity (n_b):

- Target new physics produced in association to top or bottom quarks

Scalar sum of hadronic transverse energy (H_T)

- Probes various hadronic energy scales

Backgrounds

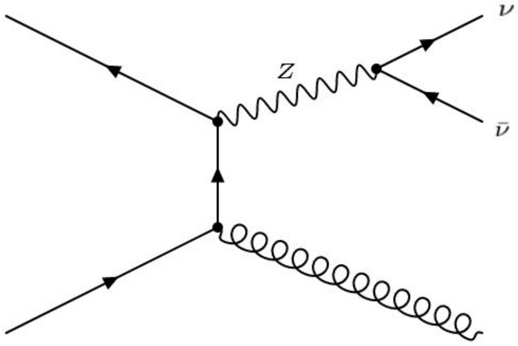

Z + jets

- Z decays invisibly

Backgrounds

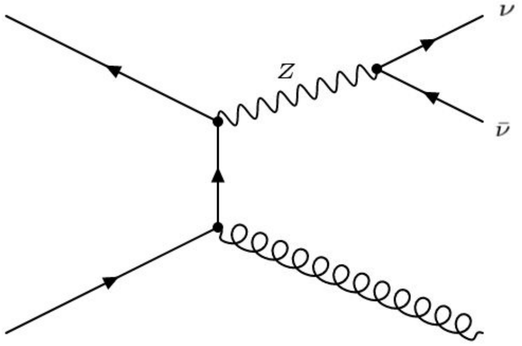

Z + jets

- Z decays invisibly

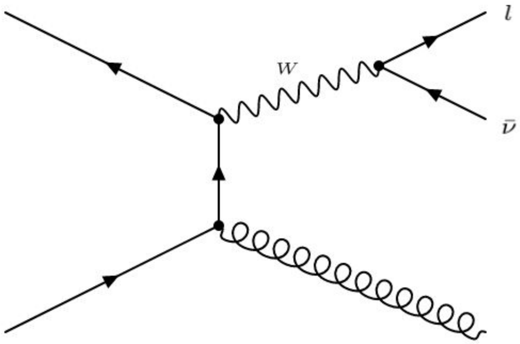

W + jets

- W decays into a hadronic tau
- W decays into e or μ which is out-of-acceptance

Backgrounds

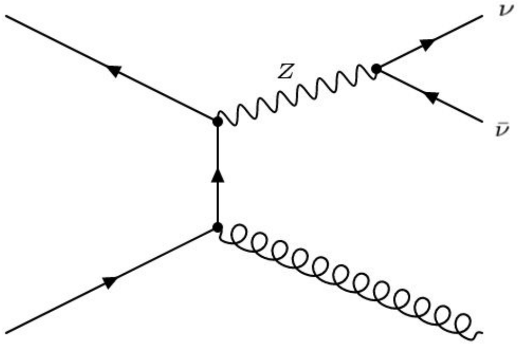

Z + jets

- Z decays invisibly

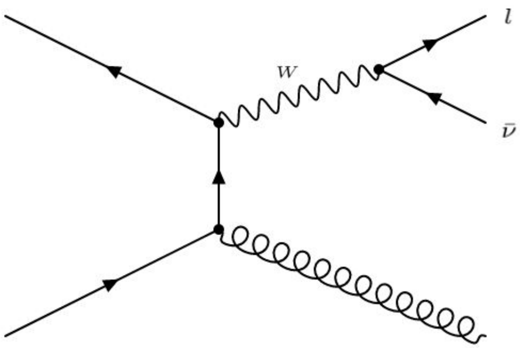

W + jets

- W decays into a hadronic tau
- W decays into e or μ which is out-of-acceptance

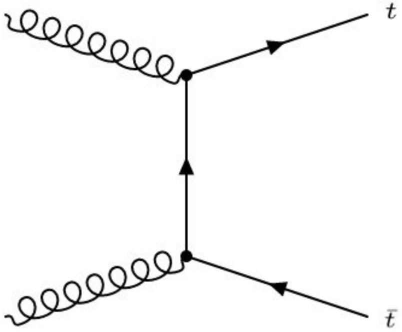

tt + jets

- Top quarks form b-jets

Backgrounds

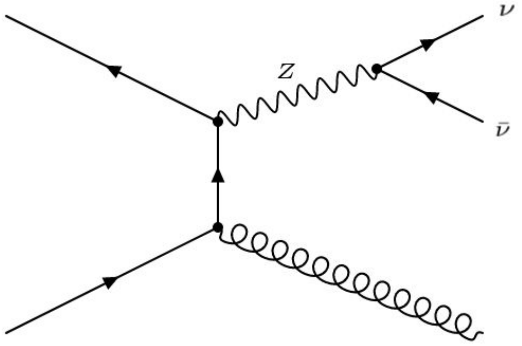

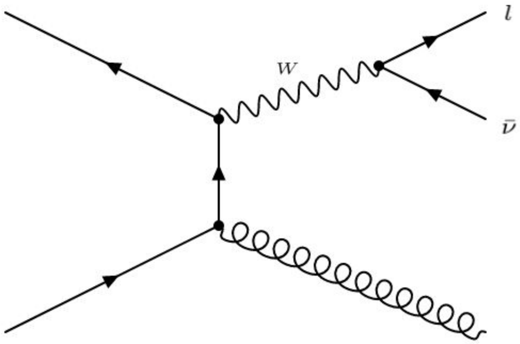

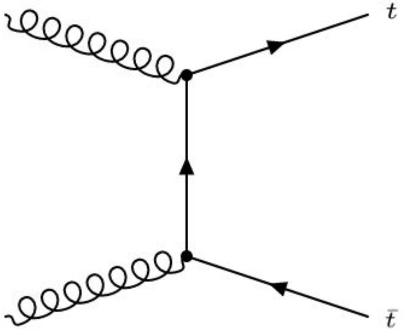

Z + jets

- Z decays invisibly

QCD

- Multijet QCD with jet mismeasurement leading to missing energy

W + jets

- W decays into a hadronic tau
- W decays into e or μ which is out-of-acceptance

tt + jets

- Top quarks form b-jets

Dedicated variables

- Cuts on dedicated variables reduce QCD multijet to a percent-level background:
  - α_T and $\Delta\phi^*_{min}$

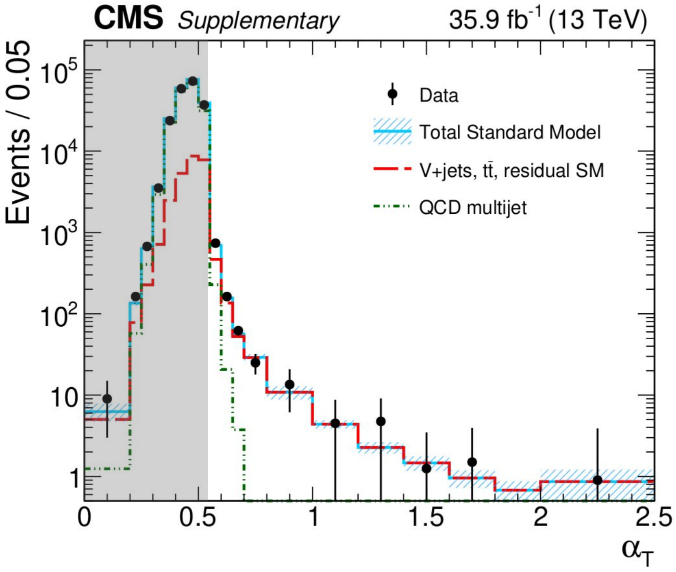

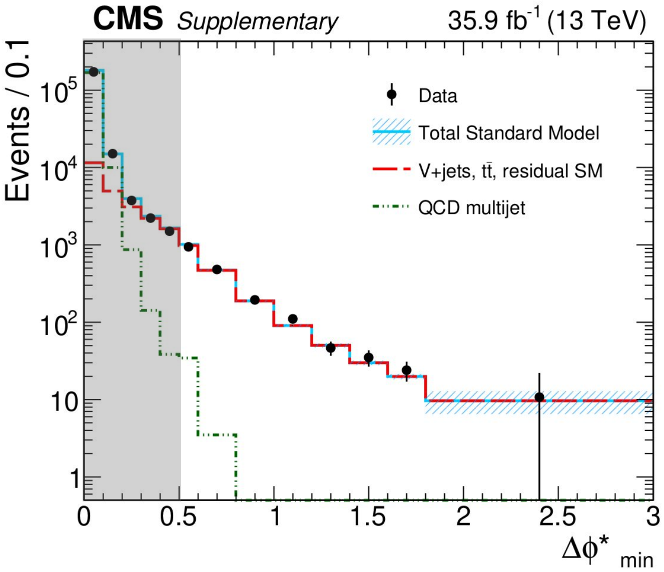

Background estimation - Electroweak

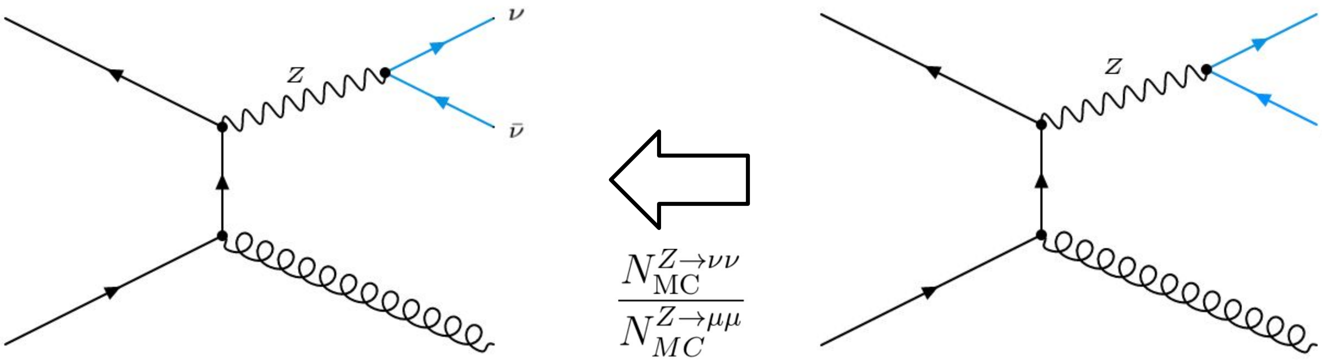

$$\frac{N^{Z\to\nu\nu}_{\mathrm{MC}}}{N^{Z\to\mu\mu}_{MC}}$$

- Use any data-MC discrepancies due to mismodelling or higher-order effects in the Z decays to muons to correct the MC prediction of Z invisible decays in the signal region
- The ratio of MC events (known as the transfer factor) results in a cancellation of some of the systematics

Background estimation - Electroweak

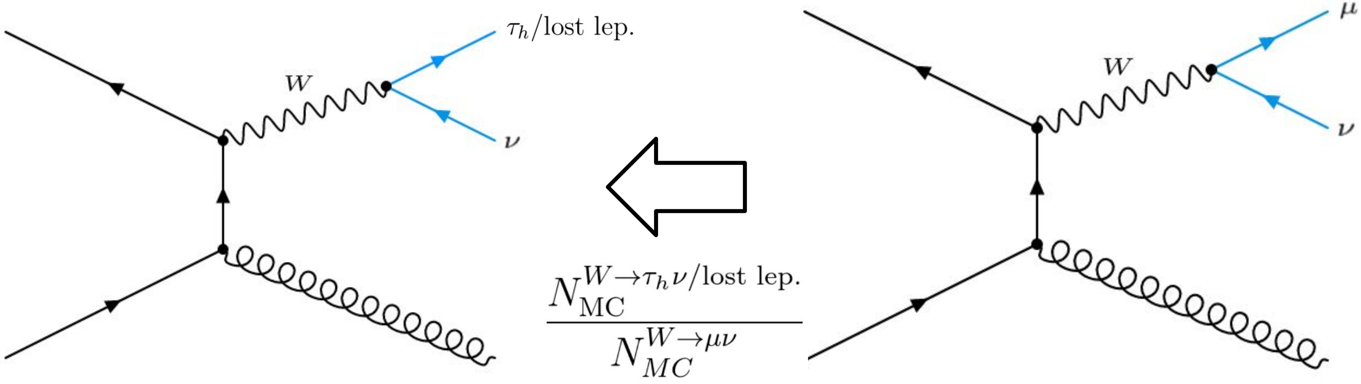

$$\frac{N_{\mathrm{MC}}^{W\to\tau_h\nu/\text{lost lep.}}}{N_{MC}^{W\to\mu\nu}}$$

- Use any data-MC discrepancies due to mismodelling or higher-order effects in the W decays to a muon to correct the MC prediction of W decays to hadronic taus or out-of-acceptance leptons in the signal region
- The ratio of MC events results in a cancellation of some of the systematics

Treatment of systematic uncertainties

- Known systematics are propagated through to every measurement (object corrections, pile-up reweighting, ...)

- Additional unknown systematics from extrapolations in the transfer factors
- For example, the dimuon region used to predict the Z invisible decays does not have an α_T cut
- To test this, compare prediction to observed event yields for α_T>0.55 predicted by the α_T<0.55 region, all in the dimuon region

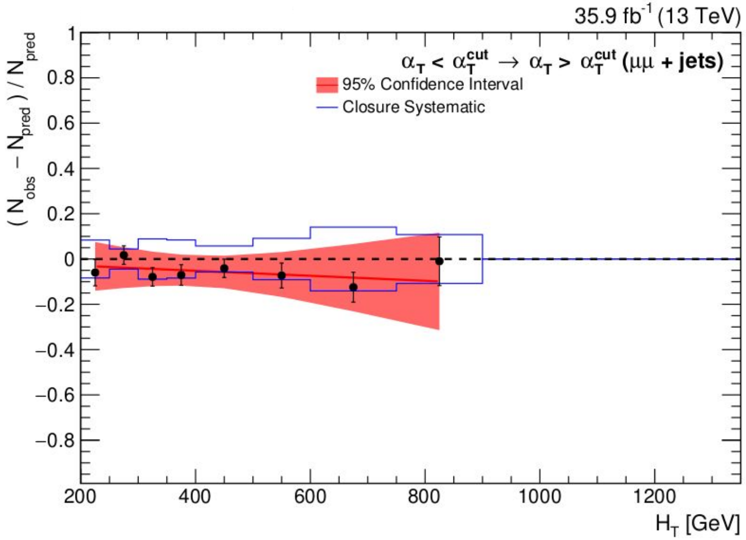

Results

- All predictions and systematics are used in a likelihood model to obtain the Standard Model expectation in the signal region
- Background prediction and data counts per analysis bin:

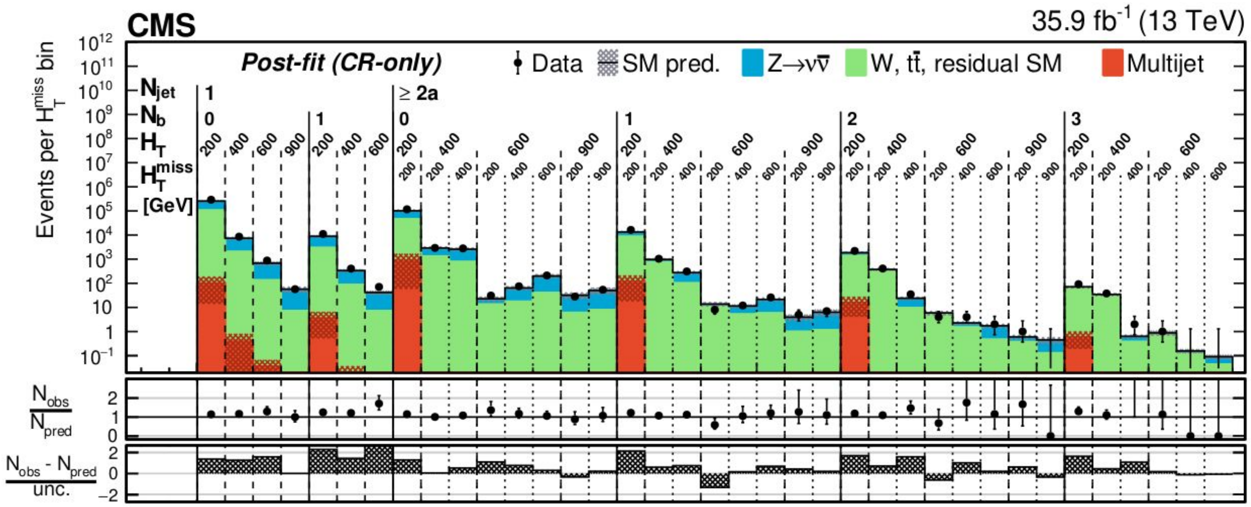

Results

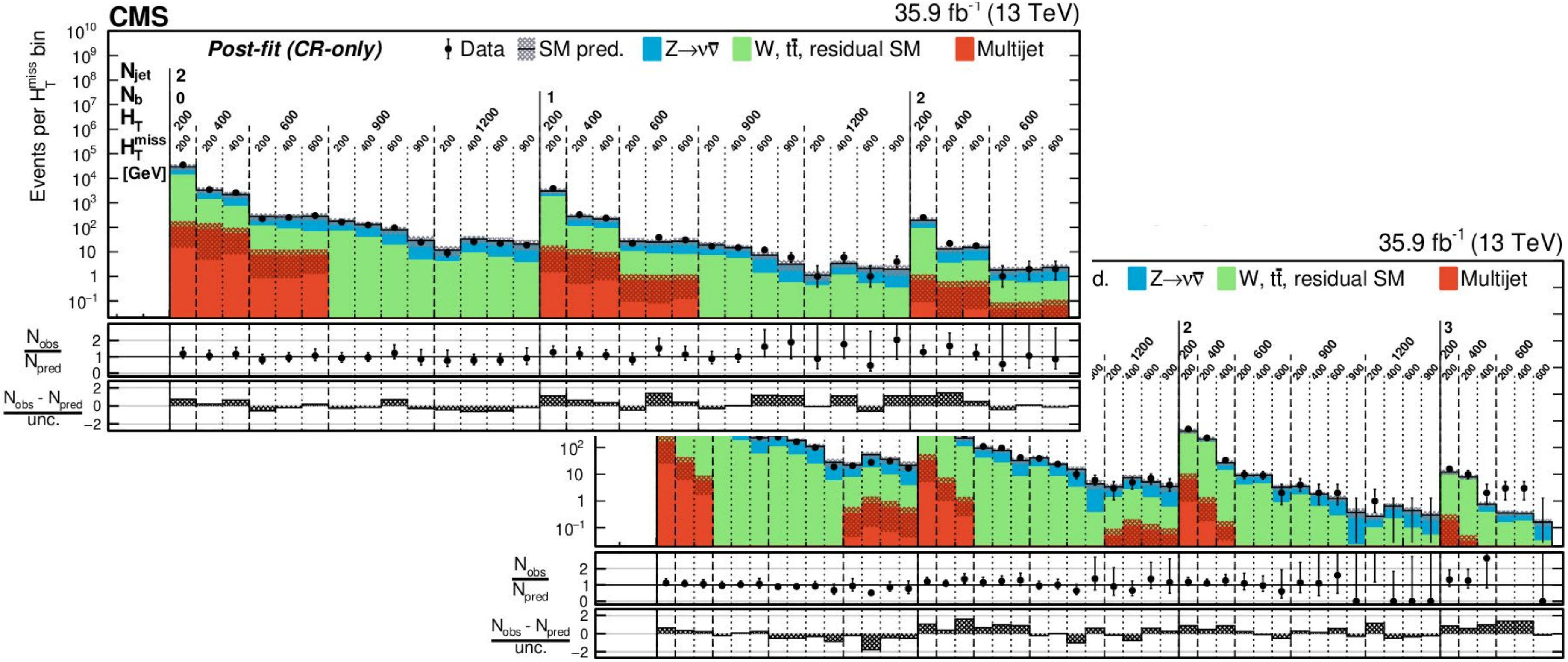
CMS
35.9 fb^{-1} (13 TeV)
Post-fit (CR-only)
Data
SM pred.
Z→νν̄
W, tt̄, residual SM
Multijet
Events per H_T^{miss} bin
N_{jet}
N_b
H_T
H_T^{miss}
[GeV]
$\frac{N_{obs}}{N_{pred}}$
$\frac{N_{obs} - N_{pred}}{unc.}$
35.9 fb^{-1} (13 TeV)
Z→νν̄
W, tt̄, residual SM
Multijet

Results

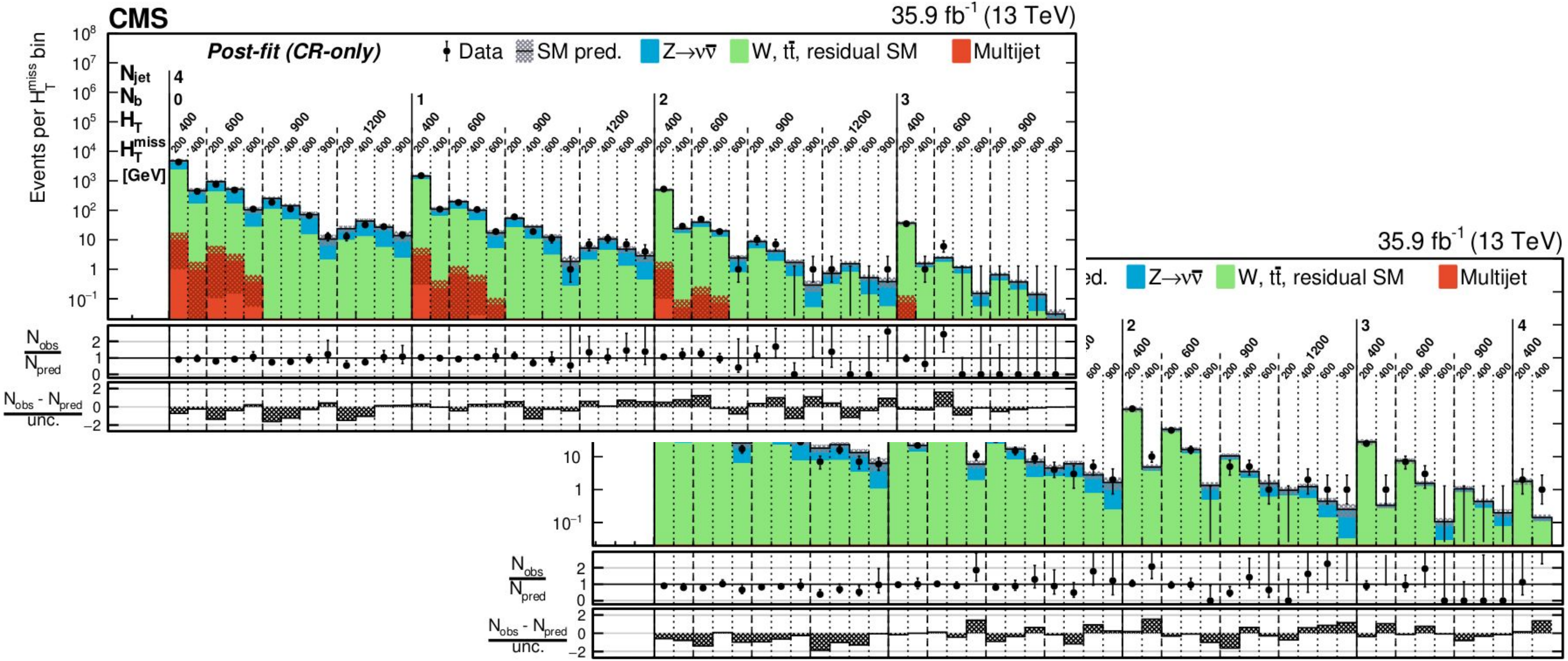
CMS
35.9 fb^{-1} (13 TeV)
Post-fit (CR-only)
Data
SM pred.
Z→νν̄
W, tt̄, residual SM
Multijet
Events per H_T^{miss} bin
N_{jet}
N_b
H_T
H_T^{miss}
[GeV]
$\frac{N_{obs}}{N_{pred}}$
$\frac{N_{obs} - N_{pred}}{unc.}$
35.9 fb^{-1} (13 TeV)

Results

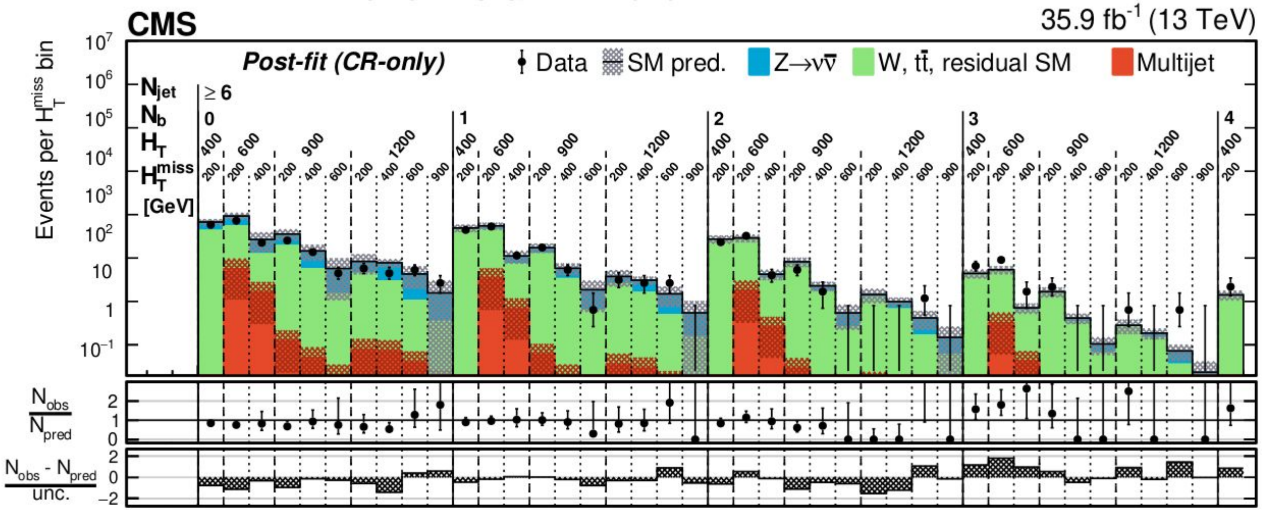
CMS
35.9 fb^{-1} (13 TeV)
Post-fit (CR-only)
Data
SM pred.
Z→νν̄
W, tt̄, residual SM
Multijet
Events per H_T^{miss} bin
N_{jet}
N_b
H_T
H_T^{miss}
[GeV]
≥ 6
0
1
2
3
4
N_{obs} / N_{pred}
N_{obs} - N_{pred} / unc.

Interpretations

- No clear evidence for new physics
- We can interpret these in the context of the simplified Dark Matter models to set a 95% upper limit on the cross section as a function the mediator and Dark Matter masses

- This is still a work-in-progress. Stay tuned

BACKUP

Dedicated variables

$$\alpha_T = \frac{1}{2} \times \frac{H_T - \Delta H_T}{\sqrt{(H_T)^2 + (H_T^{\mathrm{miss}})^2}}$$

Jet pT scalar sum

Jet pT vector sum

Effective at rejecting mismeasured QCD

- All jets are clustered into one of two pseudo-jets (where ΔH_T the energy imbalance of the two pseudo-jets, is minimised)
- Balanced events have $\alpha_T = 0.5$
- Mismeasured balanced events are strongly biased towards $\alpha_T < 0.5$
- Genuine MET events have a long-tail for $\alpha_T > 0.5$

$$\Delta\phi^{*}_{\mathrm{min}} = \min_{\forall j_k \in n_{\mathrm{jet}}} \Delta\phi\Big(-\vec{p}_T^{\,j_k}, \sum_{\substack{j_i=1 \\ j_i \neq j_k}}^{n_{\mathrm{jet}}} \vec{p}_T^{\,j_i}\Big)$$

Very robust against over-/under-measurement, as well as heavy flavour QCD

- Minimum ***Δϕ*** (over all jets) between a jet and MHT computed without that jet
- Peaked at zero, with a long tail of genuine MET events

Selection and categorization

Physics object acceptances	
Jet	$p_{\mathrm{T}} > 40\,\mathrm{GeV}$, $\lvert\eta\rvert < 2.4$
Photon	$p_{\mathrm{T}} > 25\,\mathrm{GeV}$, $\lvert\eta\rvert < 2.5$, isolated in cone $\Delta R < 0.3$
Electron	$p_{\mathrm{T}} > 10\,\mathrm{GeV}$, $\lvert\eta\rvert < 2.5$, $I^{\mathrm{rel}} < 0.1$ in cone $0.05 < \Delta R(p_{\mathrm{T}}) < 0.2$
Muon	$p_{\mathrm{T}} > 10\,\mathrm{GeV}$, $\lvert\eta\rvert < 2.5$, $I^{\mathrm{rel}} < 0.2$ in cone $0.05 < \Delta R(p_{\mathrm{T}}) < 0.2$
Single isolated track (SIT)	$p_{\mathrm{T}} > 10\,\mathrm{GeV}$, $\lvert\eta\rvert < 2.5$, $I^{\mathrm{track}} < 0.1$ in cone $\Delta R < 0.3$
Baseline event selection	
All-jet final state	Veto events containing photons, electrons, muons, and SITs within acceptance
$p_{\mathrm{T}}^{\mathrm{miss}}$ quality	Veto events based on filters related to beam and instrumental effects
Jet quality	Veto events containing jets that fail identification criteria or $0.1 < f_{\mathrm{h}^{\pm}}^{\mathrm{j}_1} < 0.95$
Jet energy and sums	$p_{\mathrm{T}}^{\mathrm{j}_1} > 100\,\mathrm{GeV}$, $H_{\mathrm{T}} > 200\,\mathrm{GeV}$, $H_{\mathrm{T}}^{\mathrm{miss}} > 200\,\mathrm{GeV}$
Jets outside acceptance	$H_{\mathrm{T}}^{\mathrm{miss}} / p_{\mathrm{T}}^{\mathrm{miss}} < 1.25$, veto events containing jets with $p_{\mathrm{T}} > 40\,\mathrm{GeV}$ and $\lvert\eta\rvert > 2.4$
Signal region	Baseline selection +
α_{T} threshold (H_{T} range)	0.65 (200–250 GeV), 0.60 (250–300), 0.55 (300–350), 0.53 (350–400), 0.52 (400–900)
$\Delta\phi_{\mathrm{min}}^{*}$ threshold	$\Delta\phi_{\mathrm{min}}^{*} > 0.5$ ($n_{\mathrm{jet}} \geq 2$), $\Delta\phi_{\mathrm{min}}^{*25} > 0.5$ ($n_{\mathrm{jet}} = 1$)

Nominal categorization schema		
n_{jet}	1	(monojet)
	$\geq 2a$	(a denotes asymmetric, $40 < p_{\mathrm{T}}^{\mathrm{j}_2} < 100\,\mathrm{GeV}$)
	2, 3, 4, 5, ≥ 6	(symmetric, $p_{\mathrm{T}}^{\mathrm{j}_2} > 100\,\mathrm{GeV}$)
n_{b}	0, 1, 2, 3, ≥ 4	(can be dropped/merged *vs.* n_{jet})
H_{T} boundaries	200, 400, 600, 900, 1200 GeV	(can be dropped/merged *vs.* n_{jet}, n_{b})
$H_{\mathrm{T}}^{\mathrm{miss}}$ boundaries	200, 400, 600, 900 GeV	(can be dropped/merged *vs.* n_{jet}, n_{b}, H_{T})
Simplified categorization schema		
Topology (n_{jet}, n_{b})	Monojet-like	$(1 \cap \geq 2a, 0)$, $(1 \cap \geq 2a, \geq 1)$
	Low n_{jet}	$(2 \cap 3, 0 \cap 1)$, $(2 \cap 3, \geq 2)$
	Medium n_{jet}	$(4 \cap 5, 0 \cap 1)$, $(4 \cap 5, \geq 2)$
	High n_{jet}	$(\geq 6, 0 \cap 1)$, $(\geq 6, \geq 2)$
H_{T} boundaries	$H_{\mathrm{T}} > 200\,\mathrm{GeV}$ ($n_{\mathrm{jet}} \leq 3$), $H_{\mathrm{T}} > 400\,\mathrm{GeV}$ ($n_{\mathrm{jet}} \geq 4$)	
$H_{\mathrm{T}}^{\mathrm{miss}}$ boundaries	200, 400, 600, 900 GeV	
Control regions	Baseline selection +	
μ+jets (inverted μ veto)	$p_{\mathrm{T}}^{\mu_1} > 30\,\mathrm{GeV}$, $\lvert\eta^{\mu_1}\rvert < 2.1$, $\Delta R(\mu, \mathrm{j_i}) > 0.5$, $30 < m_{\mathrm{T}}(\vec{p}_{\mathrm{T}}^{\mu}, \vec{p}_{\mathrm{T}}^{\mathrm{miss}}) < 125\,\mathrm{GeV}$	
$\mu\mu$+jets (inverted μ veto)	$p_{\mathrm{T}}^{\mu_{1,2}} > 30\,\mathrm{GeV}$, $\lvert\eta^{\mu_{1,2}}\rvert < 2.1$, $\Delta R(\mu_{1,2}, \mathrm{j_i}) > 0.5$, $\lvert m_{\mu\mu} - m_{\mathrm{Z}}\rvert < 25\,\mathrm{GeV}$	
Multijet-enriched	Sidebands to signal region: $H_{\mathrm{T}}^{\mathrm{miss}} / p_{\mathrm{T}}^{\mathrm{miss}} > 1.25$ and/or $\Delta\phi_{\mathrm{min}}^{*} < 0.5$	

Analysis bins

n_{jet}	n_{b}	H_{T} [GeV]				
		200	400	600	900	1200
1	0	200	400	600	900	—
1	1	200	400	600	—	—
$\geq 2a$	0	200	200, 400	200, 400, 600	200, 900	—
$\geq 2a$	1	200	200, 400	200, 400, 600	200, 900	—
$\geq 2a$	2	200	200, 400	200, 400, 600	200, 900	—
$\geq 2a$	≥ 3	200	200, 400	200, 400, 600	—	—
2	0	200	200, 400	200, 400, 600	200, 400, 600, 900	200, 400, 600, 900
2	1	200	200, 400	200, 400, 600	200, 400, 600, 900	200, 400, 600, 900
2	2	200	200, 400	200, 400, 600	—	—
3	0	200	200, 400	200, 400, 600	200, 400, 600, 900	200, 400, 600, 900
3	1	200	200, 400	200, 400, 600	200, 400, 600, 900	200, 400, 600, 900
3	2	200	200, 400	200, 400, 600	200, 400, 600, 900	200, 400, 600, 900
3	3	200	200, 400	200, 400, 600	—	—
4	0	—	200, 400	200, 400, 600	200, 400, 600, 900	200, 400, 600, 900
4	1	—	200, 400	200, 400, 600	200, 400, 600, 900	200, 400, 600, 900
4	2	—	200, 400	200, 400, 600	200, 400, 600, 900	200, 400, 600, 900
4	≥ 3	—	200, 400	200, 400, 600	200, 400, 600, 900	—
5	0	—	200, 400	200, 400, 600	200, 400, 600	200, 400, 600, 900
5	1	—	200, 400	200, 400, 600	200, 400, 600	200, 400, 600, 900
5	2	—	200, 400	200, 400, 600	200, 400, 600	200, 400, 600, 900
5	3	—	200, 400	200, 400, 600	200, 400, 600	—
5	≥ 4	—	200, 400	—	—	—
≥ 6	0	—	200	200, 400	200, 400, 600	200, 400, 600, 900
≥ 6	1	—	200	200, 400	200, 400, 600	200, 400, 600, 900
≥ 6	2	—	200	200, 400	200, 400, 600	200, 400, 600, 900
≥ 6	3	—	200	200, 400	200, 400, 600	200, 400, 600, 900
≥ 6	≥ 4	—	200	—	—	—

Systematic uncertainties on transfer factors

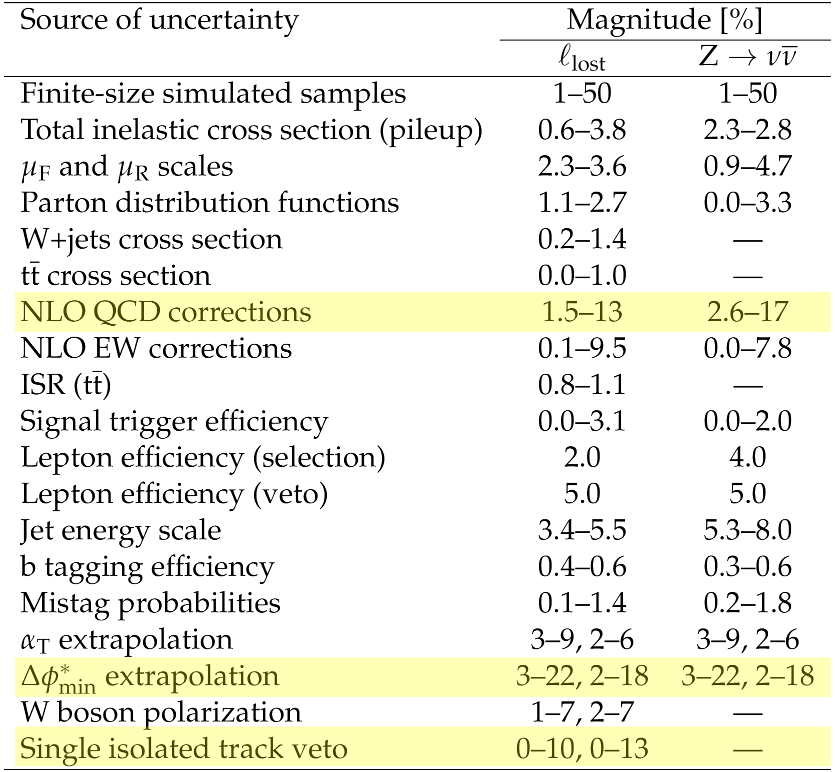

Source of uncertainty	Magnitude [%]	
	ℓ_{lost}	$Z \to \nu\bar{\nu}$
Finite-size simulated samples	1–50	1–50
Total inelastic cross section (pileup)	0.6–3.8	2.3–2.8
μ_{F} and μ_{R} scales	2.3–3.6	0.9–4.7
Parton distribution functions	1.1–2.7	0.0–3.3
W+jets cross section	0.2–1.4	—
$\mathrm{t\bar{t}}$ cross section	0.0–1.0	—
NLO QCD corrections	1.5–13	2.6–17
NLO EW corrections	0.1–9.5	0.0–7.8
ISR ($\mathrm{t\bar{t}}$)	0.8–1.1	—
Signal trigger efficiency	0.0–3.1	0.0–2.0
Lepton efficiency (selection)	2.0	4.0
Lepton efficiency (veto)	5.0	5.0
Jet energy scale	3.4–5.5	5.3–8.0
b tagging efficiency	0.4–0.6	0.3–0.6
Mistag probabilities	0.1–1.4	0.2–1.8
α_{T} extrapolation	3–9, 2–6	3–9, 2–6
$\Delta\phi^{*}_{\mathrm{min}}$ extrapolation	3–22, 2–18	3–22, 2–18
W boson polarization	1–7, 2–7	—
Single isolated track veto	0–10, 0–13	—